

Nanozyme linked multi-array gas driven sensor for real-time quantitative detection of *Group A streptococcus*

Qi Wang^{1†}, Pei Liu^{2†}, Ke Xiao³, Wenyng Zhou¹, Jinfeng Li^{4*}, Yun Xi^{1*}

¹ Department of Laboratory Medicine, The Third Affiliated Hospital, Sun Yat-sen University, Guangzhou 510630, China;

² Department of Neurosurgery, Ningguo People's Hospital, Xuancheng 242300, China;

³ Department of Laboratory Medicine, The Second Hospital of Chinese Medicine in Guangdong, Guangzhou, 510095, China;

⁴ Shenzhen Bao'an District Central Blood Station, Shenzhen 518101, China.

† These authors contributed equally to this work.

* To whom correspondence should be addressed: xiyun1993@163.com (Y Xi); or shandongli518@126.com (J Li)

Contents

Fig. S1. Assembly of NLMAGS components.

Fig. S2. Stability of NLMAGS.

Fig. S3. The influence of different environmental temperatures on determination.

Fig. S4. Optimization.

Fig. S5. Schematic and sensitivity of Au@Pt@PdNPs-LFIA for detection of GAS.

Fig. S6. The optimization of mAb1 concentration coated in ELISA.

Fig. S7. The optimization of mAb2-HRP dilution times in ELISA.

Fig. S8. Sensitivity of the ELISA for detecting GAS.

Table S1. The internal diameter and external diameter of valve and capillary.

Table S2. Different concentrations of *GAS* standard were detected using NLMAGS.

Table S3. As of the completion date (03-Jun-2024) of this work, the cost of materials for assembly of NLMAGS.

Table S4. The detection results of spiked samples between ELISA and NLMAGS.

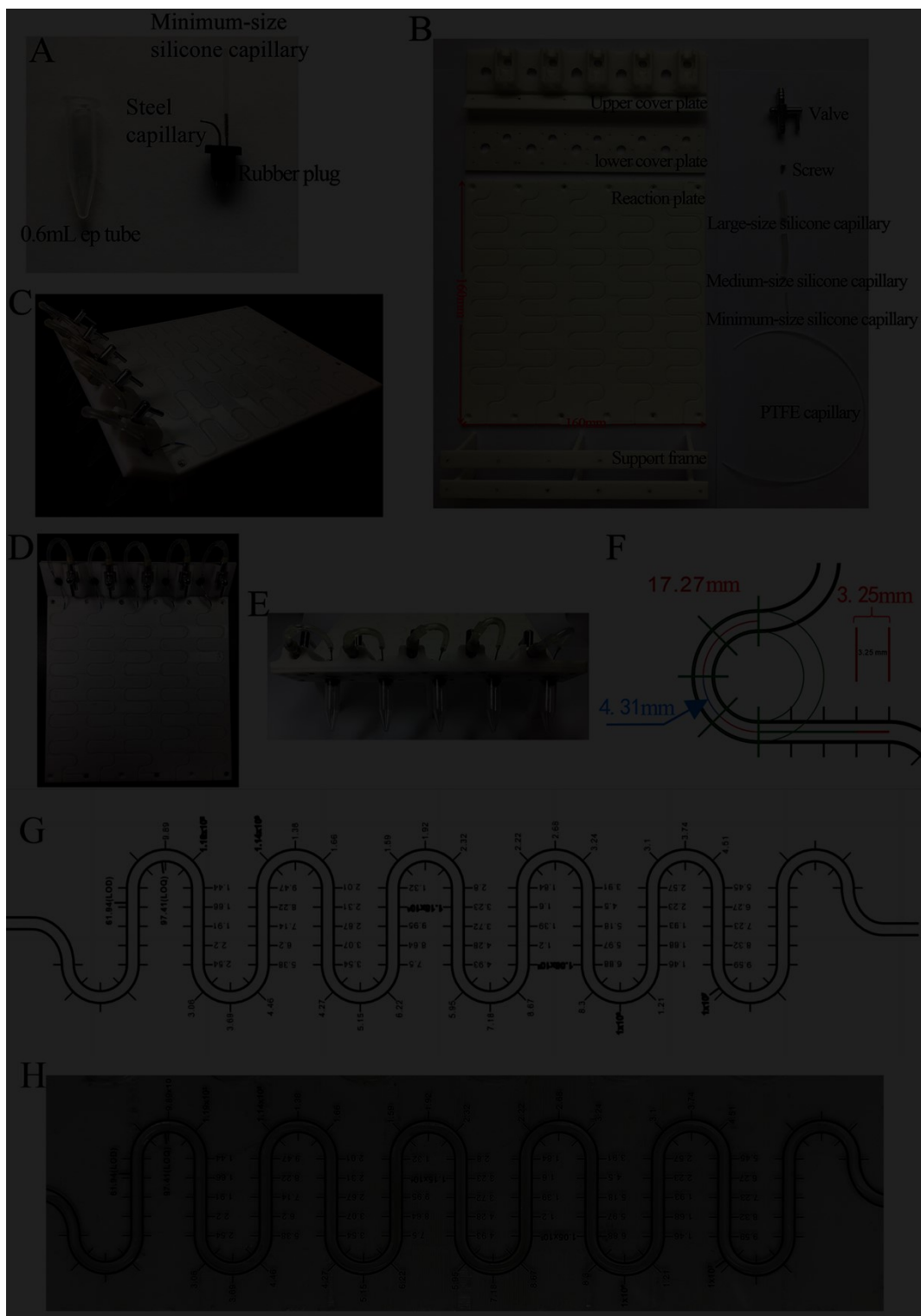


Fig. S1. Assembly of NLMAGS components. **(A)** Detailed components of the reaction device; **(B)** Detailed components of the result reading device; **(C)** The side view of NLMAGS; **(D)** The vertical view of NLMAGS; **(E)** The front view of NLMAGS; **(F)** The size of the reading ruler; **(G)** The design of reading ruler; **(H)** The

image of reading ruler.

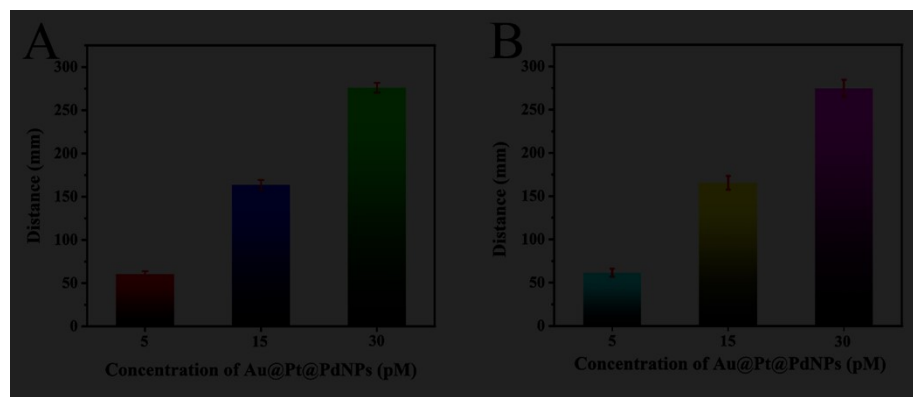


Fig. S2. Stability of NLMAGS. **(A)** The intra-assay of the NLMAGS ($n=5$); **(B)** The inter-assay of the NLMAGS ($n=5$).

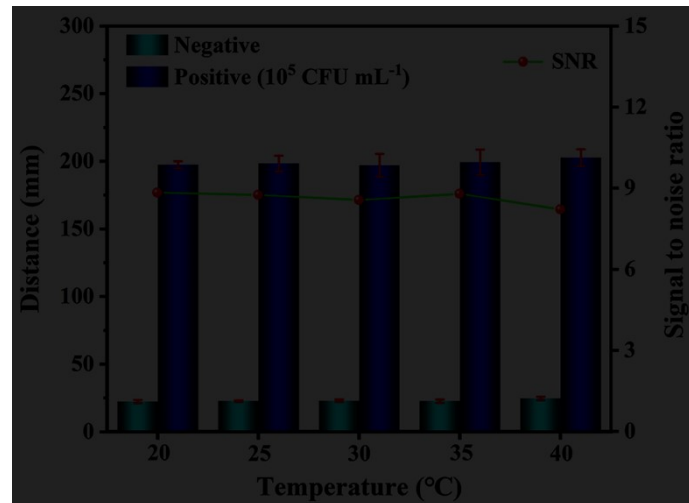


Fig. S3. The influence of different environmental temperatures on determination.

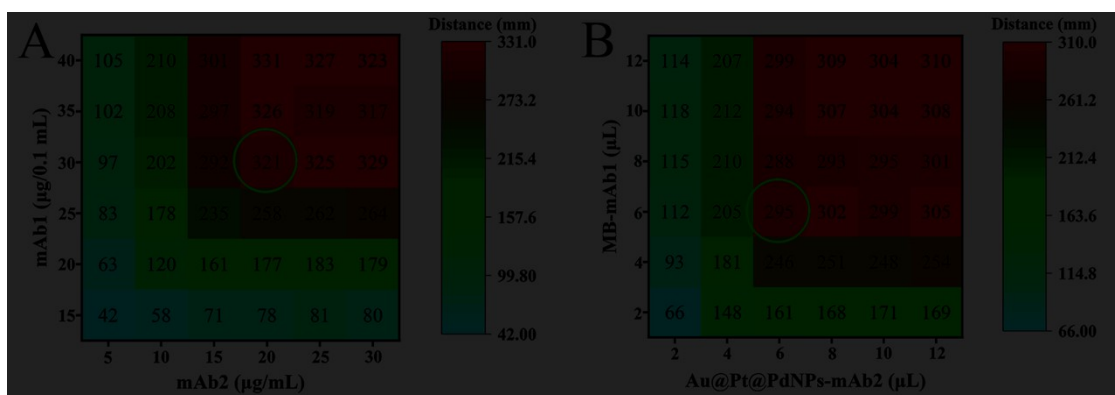


Fig. S4. Optimization. **(A)** Different amount of mAb1 (15, 20, 25, 30, 35, or 40 µg) labeled 0.1 mL magnetic beads and different amount of mAb2 (5, 10, 15, 20, 25, or 30 µg) labeled 1 mL Au@Pt@PdNPs were randomly paired for detecting GAS (10^7 CFU mL $^{-1}$); **(B)** Different usage of MB-mAb1 (2, 4, 6, 8, 10, 12 µL) and Au@Pt@PdNPs-mAb2 (2, 4, 6, 8, 10, 12 µL) were randomly paired for detecting GAS (10^7 CFU mL $^{-1}$).

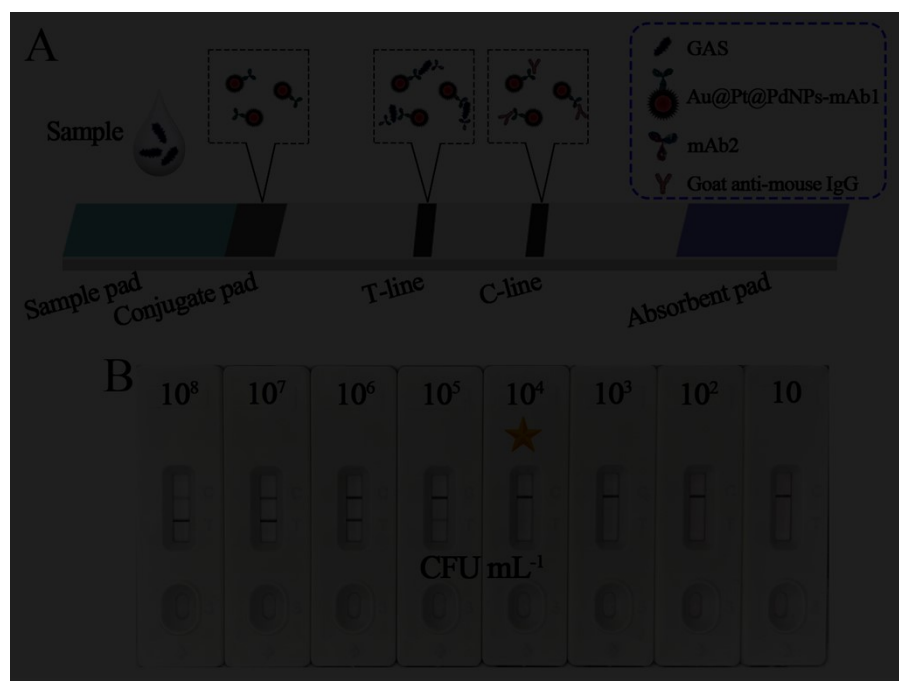


Fig. S5. Schematic and sensitivity of Au@Pt@PdNPs-LFIA for detection of *GAS*. **(A)** The Schematic of Au@Pt@PdNPs-LFIA; **(B)** The sensitivity of Au@Pt@PdNPs-LFIA for detection of *GAS*.

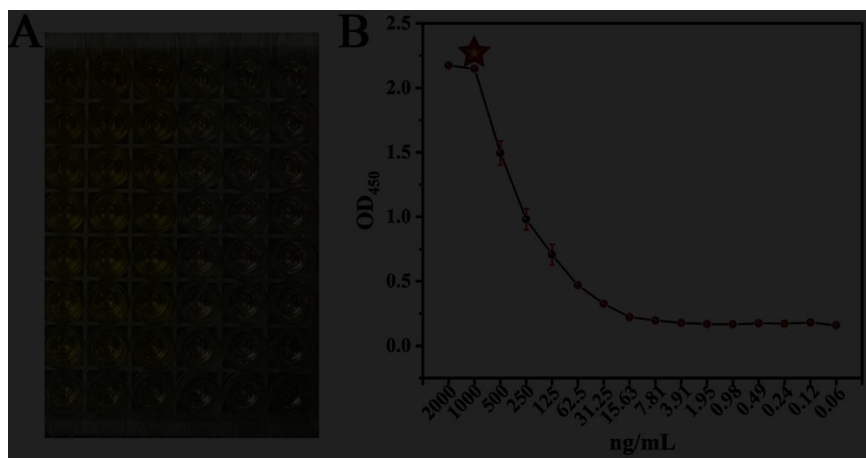


Fig. S6. The optimization of mAb1 coating concentration in ELISA. **(A)** ELISA coated with different concentrations (0.06-2000 ng/mL) of mAb1 for GAS (10^7 CFU mL⁻¹) detection. **(B)** The OD values corresponding to the different concentration (0.06-2000 ng/mL) of mAb1 coated in ELISA.

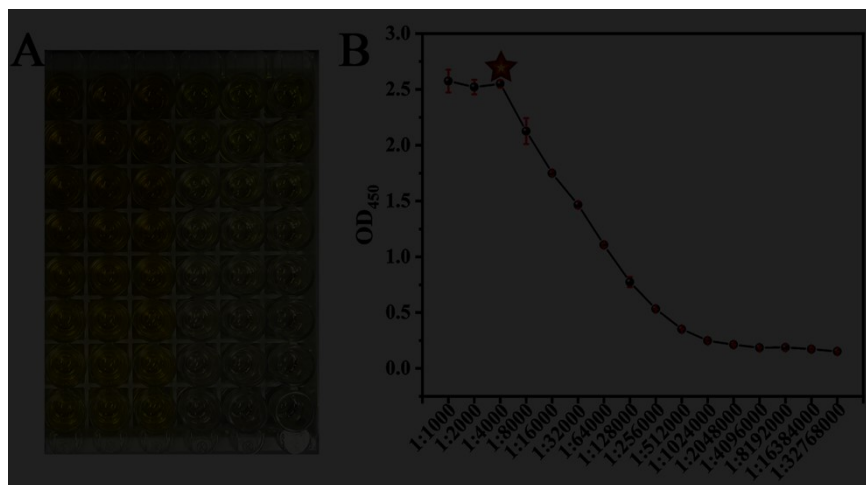


Fig. S7. The optimization of mAb2-HRP dilution times in ELISA. **(A)** ELISA worked with different dilution times (1000- 32768000 times) of mAb2-HRP for GAS (10^7 CFU mL⁻¹) detection. **(B)** The OD values corresponding to the different dilution times (1000- 32768000 times) of mAb2-HRP used in ELISA.

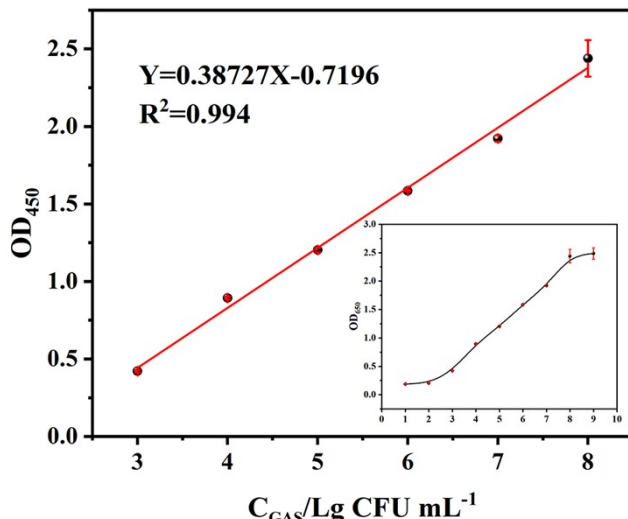


Fig. S8. The quantitative curve of ELISA.

Table S1. The internal diameter and external diameter of the valve and capillary

	Internal diameter (mm)	External diameter (mm)
Valve	3.5	4
Large-size silicone capillary	2.00	4.00
Medium-size silicone capillary	1.00	3.00
Minimum-size silicone capillary	0.50	1.50
Steel capillary	0.65	0.80
PTFE (polytetrafluoroethylene) capillary	0.50	0.90

Table S2. Different concentrations of *GAS* standard were detected using NLMAGS

	Test 1 (mm)	Test 2 (mm)	Test 3 (mm)	Average (mm)	SD	CV (%)
Negative	17	18	20	18.33	1.25	6.8
10	19	20	21	20	0.82	4.08
10²	40	35	34	36.33	2.62	7.22
10³	92	87	78	85.67	5.79	6.76
10⁴	162	148	147	152.33	6.85	4.5
10⁵	192	210	215	205.67	9.88	4.8
10⁶	265	249	245	253	8.64	3.42
10⁷	303	302	282	295.67	9.67	3.27
10⁸	340	317	332	329.67	9.53	2.89
10⁹	347	331	346	341.33	7.32	2.14

Average: Average of movement distance (mm) detected using the NLMAGS (n=3).

SD: Standard deviation of movement distance (mm) detected using the NLMAGS (n=3). (**CV**, Coefficient of Variation) = (SD/ Average)*100%.

Table S3. As of the completion date (03-Jun-2024) of this work, the cost of materials

for assembly of NLMAGS.

Reusable material	Cost (\$)/test	One-time material	Cost (\$)/test
3D printing consumables	0.2	PTFE capillary	0.06
Valve	0.43	Monocloning antibody	0.2
Large-size silicone capillary	0.002	Magnetic bead	0.1
Medium-size silicone capillary	0.002	Au@Pt@PdNPs	0.02
Minimum-size silicone capillary	0.001	Others	0.1
Steel capillary	0.02	Total	
Rubber plug	0.23		0.48
Reading ruler (Film material)	0.2		
Total	1.085		

Table S4. The detection results of spiked samples between ELISA and NLMAGS

Sample number	ELISA measurement (n=3)						NLMAGS measurement (n=3)					
	Test 1 (CFU mL ⁻¹)	Test 2 (CFU mL ⁻¹)	Test 3 (CFU mL ⁻¹)	Average (CFU mL ⁻¹)	SD	CV (%)	Test 1 (CFU mL ⁻¹)	Test 2 (CFU mL ⁻¹)	Test 3 (CFU mL ⁻¹)	Average (CFU mL ⁻¹)	SD	CV (%)
1	29458	31157	28375	29663	1145	3.86	28000	32000	32300	30767	1960	6.37
2	9387	9528	10463	9793	477	4.88	9950	11500	11500	10983	731	6.65
3	158236	153565	165898	159233	5084	3.19	184000	160000	184000	176000	11314	6.43
4	1023	981	1161	1055	77	7.29	1140	1140	1380	1220	113	9.27
5	1422	1589	1603	1538	82	5.35	1380	1660	1380	1473	132	8.96
6	30785	31956	29482	30741	1010	3.29	32300	28000	32300	30867	2027	6.57
7	84629	84051	78104	82261	2949	3.59	86700	86700	105000	92800	8627	9.3
8	2493	2526	2154	2391	168	7.03	3070	2670	3070	2937	189	6.42
9	1653	1733	1508	1631	93	5.71	1140	1380	1140	1220	113	9.27
10	17453	16298	16949	16900	473	2.8	13200	15900	15900	15000	1273	8.49
11	2519	2632	2841	2664	133	5.01	2670	3070	3540	3093	356	11.49

12	4418	4917	4537	4624	213	4.6	4270	5150	5150	4857	415	8.54
13	55813	59640	60119	58524	1927	3.29	59500	59500	71800	63600	5798	9.12
14	7920139	8014752	7613501	7849464	171264	2.18	7230000	7230000	8320000	7593333	513831	6.77
15	21368907	23165889	21586916	22040571	800682	3.63	11600000	9590000	11600000	10930000	947523	8.67
16	79264	74645	79158	77689	2153	2.77	71800	86700	86700	81733	7024	8.59
17	1182	1234	1035	1150	84	7.33	1380	1140	1380	1300	113	8.7
18	640675	632238	562467	611793	35049	5.73	597000	688000	597000	627333	42898	6.84
19	26033	26846	28459	27113	1008	3.72	23200	23200	28000	24800	2263	9.12
20	37156	39578	36412	37715	1352	3.58	32300	37200	42800	37433	4290	11.46
21	448	371	465	428	41	9.56	538	369	446	451	69	15.32
22	42962	41194	44646	42934	1409	3.28	42800	42800	49300	44967	3064	6.81
23	5929	6847	6457	6411	376	5.87	7500	6220	7500	7073	603	8.53
24	84256	91757	89521	88511	3144	3.55	86700	105000	86700	92800	8627	9.29

Average: Average of results detected using the ELISA or NLMAGS (n=3). **SD:** Standard deviation of results detected using the ELISA or NLMAGS (n=3). **(CV, Coefficient of Variation) = (SD/ Average)*100%.**